Persistent photo-excitation in $GdBa_2Cu_3O_{6.5}$ in a simultaneous Raman and electrical-transport experiment

S. Bahrs,[1] J. Guimpel,[2] A. R. Goñi,[3] B. Maiorov,[4] A. Fainstein,[2] G. Nieva,[2] and C. Thomsen[1]
[1]*Institut für Festkörperphysik, Technische Universität Berlin, Hardenbergstr. 36, 10623 Berlin, Germany*
[2]*Centro Atómico Bariloche, Comisión Nacional de Energía Atómica, 8400 San Carlos de Bariloche, Río Negro, Argentina*
[3]*ICREA Research Professor, Institut de Ciència de Materials de Barcelona, Campus de la UAB, 08193 Bellaterra, Spain*
[4]*Superconductivity Technology Center, MS K763, Los Alamos National Laboratory, Los Alamos, New Mexico 87545, USA*
(Received 28 April 2005; revised manuscript received 12 July 2005; published 3 October 2005)

We investigate the connection between persistent illumination-induced effects in underdoped $RBa_2Cu_3O_{7-\delta}$ known as persistent photoconductivity and Raman bleaching. Despite the long-standing assumption that the electrical and optical properties respond to the same light-induced change in the material, they have not been directly compared until now. We present a simultaneous experiment of Raman spectroscopy and electrical transport under visible illumination at low temperatures. The time dependence of the response in the two methods differs by two orders of magnitude, showing that the effects are connected but not identical. We discuss our results within the oxygen-vacancy reordering model of photobleaching and find that different Cu-O chain lengths affect the optical and the electrical response differently. Raman bleaching and persistent photoconductivity thus provide a different perspective on the microscopic oxygen vacancy distribution.

DOI: 10.1103/PhysRevB.72.144501 PACS number(s): 74.72.Bk, 78.30.−j, 63.50.+x, 73.50.Pz

I. MOTIVATION

Persistent photoconductivity in the $RBa_2Cu_3O_{7-\delta}$ (R=Y or rare-earth atom) family of high-temperature superconductors has been discussed in the literature for several years now.[1–5] This illumination-induced decrease in resistivity has been traced over time scales of many hours and shown to be persistent at temperatures below 250 K. At room temperature it relaxes back to equilibrium, though it does not cancel out with the aging effect in quenched samples.[3] It occurs in all oxygen-deficient samples including the insulating specimens, but is absent or very weak in the fully oxygenated compound.[6] It is also present for all choices of rare-earth atoms investigated so far, though it is specific to the material family, which features (broken) Cu-O atom chains in the nonsuperconducting basal plane of the unit cell. In superconducting samples, the critical temperature is affected, providing an interesting link to the continuous and reversible manipulation of superconducting properties via a light-induced change of doping level. The effect was found for illumination in both the superconducting and the normal states alike.[5]

All these properties put persistent photoconductivity next to light-induced effects found in the optical response of $RBa_2Cu_3O_{7-\delta}$, such as Raman-mode bleaching and the change detected in the dielectric function by reflectance anisotropy spectroscopy.[7,8] In Raman spectroscopy, in particular, defect-induced peaks typical of oxygen-deficient samples lose intensity under prolonged illumination in all investigated rare-earth compounds.[9] Their selection rules connect them to the Cu-O chain plane, as they are apparent in the spectra only for light polarized along the chains.[7,10–12] Their intensity change is also persistent at low temperature, but reversible at room temperature,[7] and it occurs independent of the superconducting or normal state of the sample in a temperature dependent study of the bleaching.[13]

Despite the wealth of experimental data the discussion about the underlying mechanism of photoinduced change has not been concluded. All suggested models involve an electronic excitation connected to the chain structure, but some rely on the trapping of electrons at oxygen vacancy sites, while others propose a structural change: photoinduced oxygen diffusion or photoassisted oxygen reordering.[2–4] The Raman bleaching effect has also been discussed in electronic and structural models.[10,11,13–16]

Though a connection of photoinduced effects in electrical transport and optical spectroscopy has long been assumed, it has never been explicitly studied. Direct comparison of published data from different optical and electrical experiments is difficult because of the many parameters involved. We took the opportunity to look at photoinduced effects from different experimental viewpoints, and performed a study where Raman spectra and transport data were acquired simultaneously in a combined setup, using identical illumination.

In this paper we present results of time-dependent Raman and transport data under illumination at five different temperatures. The temperature dependences are discussed. We find a difference of two orders of magnitude between the time constants of Raman bleaching and resistivity change. Within the oxygen reordering model, a Monte Carlo model calculation of chain fragment evolution is used to discuss the relation between different time constants and the development of Cu-O chains.

II. EXPERIMENTAL SETUP

In order to confine the electrical current through the sample to a cross section penetrated by the light of the Raman focus, we used a thin film of $GdBa_2Cu_3O_{6.5}$ instead of a bulk sample. The film was approximately 1500 Å thick. It was patterned lithographically to provide a narrow bridge of sample material (250 μm), which was covered by the Raman focus (diameter 250±10 μm), as well as contacts for a four

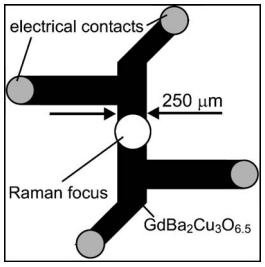

FIG. 1. Schematic view of the sample geometry.

point probe (see Fig. 1). The sample was oxygen-reduced using the corresponding temperature and oxygen pressure values for bulk samples. From the curve of resistivity versus temperature in Fig. 2(a) can be seen that the film is superconducting with an onset temperature of 30 K. By comparison to the critical temperatures of a set of other $GdBa_2Cu_3O_{7-\delta}$ films we determine the oxygen concentration to be 6.5 ± 0.1, close to the superconducting/insulating transition and in the ortho-II region of the phase diagram.[17]

A closed-cycle He cryostat with an optical window provided the cooling. The Raman spectra were recorded using a triple Jobin-Yvon T64000 spectrometer equipped with a liquid-N_2-cooled charge-coupled-device camera. Spectra were collected in backscattering geometry, accumulating two times 15 s for each spectrum.

As a light source, both for illumination of the transport experiment as well as for excitation of the Raman spectra, we used the 568 nm line of an Ar-Kr-ion laser. The focus was placed on the conducting bridge of the sample with special care taken to cover the entire strip width. Due to this, there is some background signal from beyond the edges of the sample bridge in the spectra. The power applied in all series was 7.8 mW, leading to a power density of $(15.9 \pm 1.3) \mathrm{W/cm^2}$ on the sample surface.

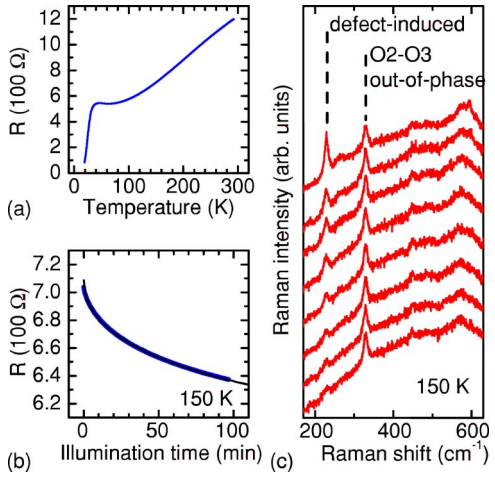

FIG. 2. (Color online) (a) Resistivity vs temperature in the non-illuminated film of $GdBa_2Cu_3O_{6.5}$ and (b) resistivity under illumination with laser light at 150 K (blue). The fit is a stretched exponential function (black). (c) Raman spectra taken sequentially with the same laser excitation, starting at the top (off-set). Each curve displayed represents an average over five spectra, with 150 s total accumulation time. While the Raman-allowed mode at 329 $\mathrm{cm^{-1}}$ is stable, the defect-induced mode at 229 $\mathrm{cm^{-1}}$ is quenched.

After each run, the sample was warmed to 300 K and kept there for at least 1 h to ensure sufficient relaxation between different temperature measurements.

III. RESULTS

Experimental data from the simultaneous Raman and transport setup is displayed in Fig. 2. Panel (a) shows the resistivity versus temperature curve of the unilluminated film. The curve indicates metallic behavior with a low T_c onset of 30 K, which is expected for an oxygen-reduced, superconducting sample near the transition to the insulating regime of the phase diagram. Estimates of the specific resistivity from the sample and contact geometry yield about 500 $\mu\Omega$ cm at 150 K, which is a typical value for oxygen-reduced films with $\delta \approx 0.5$.[1,3]

Figure 2(b) and 2(c) show an example of the effect of illumination on the sample at a temperature of 150 K. The resistivity curve (b) starts at the 150 K value of the unilluminated curve in (a) and decreases during the 90 min laser illumination period by 9%. In the same period of time, sequential Raman spectra were collected using the laser illumination for excitation. Figure 2(c) has the first spectra offset to the top of the picture, with illumination time increasing towards the bottom. The Raman-allowed mode at 329 $\mathrm{cm^{-1}}$ is the so-called pseudo-B_{1g} attributed to out-of-phase oxygen vibrations in the superconducting planes.[18] It does not change intensity or position throughout the experiment. In contrast, the peak at 229 $\mathrm{cm^{-1}}$ loses intensity and almost vanishes in the background towards the end of the sequence. This peak belongs to a group occurring exclusively for underdoped material and showing a resonance around 2.2 eV, which is connected to the Cu-O chain elements in the basal plane of the $RBa_2Cu_3O_{7-\delta}$ unit cell.[7] Several related peaks are seen around 260 and just below 600 $\mathrm{cm^{-1}}$. From Raman-bleaching studies carried out on a $YBa_2Cu_3O_{7-\delta}$ single crystal with the same excitation energy we know that at least seven defect-induced peaks can be identified between 200 and 600 $\mathrm{cm^{-1}}$ and that they all decrease at the same rate.[11,19] This indicates that all vibrations involved become Raman active by coupling to the same resonant excitation. For the present study the strongest peak at 229 $\mathrm{cm^{-1}}$ was fitted with a Lorentzian line shape and its intensity plotted in Fig. 3.

The solid line in Fig. 2(b) represents a fit with a stretched exponential function, which is commonly used to describe relaxation processes in heavily disordered systems with a dispersion of relaxation times:[20]

$$I(t) = I_0 \exp\left[-\left(\frac{t}{\tau}\right)^{\beta}\right] + \text{const.} \qquad (1)$$

Resistivity and Raman-intensity decrease in high T_c compounds have frequently been described with this function before, and we extract from it the time constants τ. For unambiguousness and simplicity of comparison, we fixed β to 0.5 in all experimental curves, the value of β which gave us the best fit to Raman bleaching and transport curves with a single exponent.

The full set of time-dependent experimental data is shown in Fig. 3, with the resistivity decrease in the upper panels and

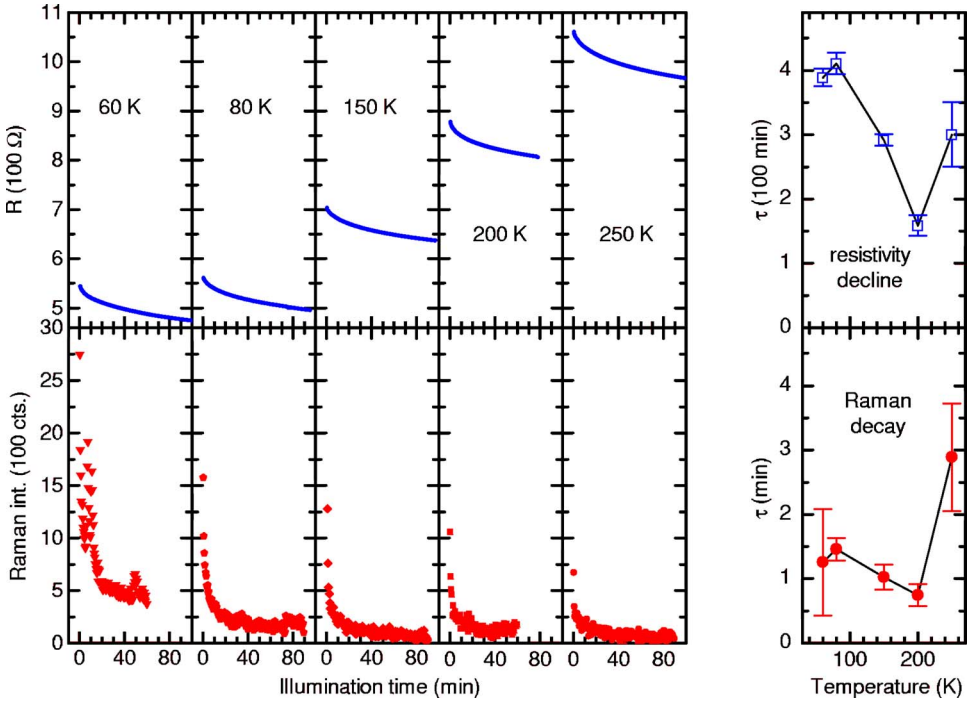

FIG. 3. (Color online) Simultaneous decrease of resistivity (upper panels, blue) and Raman intensity of the peak at 229 cm^{-1} (lower panels, red) at various temperatures in an illuminated thin film of $GdBa_2Cu_3O_{7-\delta}$. The rightmost panels show the corresponding time constants according to Eq. (1) with the exponent β fixed to 0.5.

the Raman intensity loss in the lower panels for illumination series at different temperatures. Time constants τ from stretched-exponential fits to the curves are plotted versus temperature in the rightmost panels.

The resistivity decrease starts at higher values for higher temperatures, as expected from the resistivity of the unilluminated curve [Fig. 2(a)]. In accordance with previous findings, the photoinduced change becomes faster with increasing temperature.[5] At 250 K, the highest temperature investigated, τ increases somewhat. This can be due to relaxation effects known to set in in this temperature range.[2,4] The Raman intensity decrease shows a similar development of τ vs T, with a minimum at 200 K and subsequently a pronounced increase. This is in agreement with previous studies on temperature-dependent Raman bleaching, where the most efficient decrease occurred around 190 K.[11,13] However, the error of the fit at 250 K is large because of the limited time resolution of the spectra. At 60 K, we observed fluctuations in the Raman intensity caused by very small shifts of the Raman-focus position, resulting in another large error for this fit. Except at 60 K, Raman intensity decreases to background levels within the duration of the experiment.

The most striking result of our experiment is the large difference in absolute time constants in Raman and transport: The Raman-intensity decrease is faster than the reduction of the resistivity by roughly two orders of magnitude. This raises the question whether or not both effects have the same microscopical origin.

We discuss first a technical aspect of the two measurements and its influence on the time constants. There is a technical difference between Raman spectroscopy, which probes the illuminated volume, and electrical current, which can also access unilluminated areas of the sample. The width of 250 μm of the conducting bridge was covered by the Raman focus on the surface sample (see Fig. 1). However, the film was 150 nm thick and though it was still transparent to the eye, the power density decreases exponentially between the surface and the lower layers due to absorption. Thus, while lower lying layers receive lower power density and contribute less to the Raman signal, all layers contribute to the resistivity regardless of illumination and the according time-dependent change. If the resistivity decreases according to a stretched exponential function in the illuminated volume, but has also constant, parallel contributions, the time constant extracted from a fit to the overall resistivity will be perturbed. For an estimate of the upper boundary of this effect we simply take the film to be half-illuminated (based on a penetration depth of 85 nm at $\lambda = 568$ nm from derived from an ellipsometric study on YBCO with $T_c = 66$ K in Ref. 21). We model the influence of any unperturbed contribution by a constant resistor in parallel with the time dependent one. The latter is described with a stretched exponential [Eq. (1), $\beta = 0.5$], and the combined resistivity function is fitted to the resistivity data taken under illumination at 150 K. We obtain a reduction in τ by a factor of 4. From the best fit to the data with the parallel resistor, we obtain a slightly larger share of constant resistivity with τ diminished by a factor of 8. Thus, part of the difference in the time constants may be due to the reduced illumination closer to the sample-substrate interface, but even the upper estimate of this technical aspect cannot account for the observed two orders of magnitude alone.

We will now discuss the remaining difference of over one order of magnitude in terms of the microscopic origin of photoinduced effects in underdoped $RBa_2Cu_3O_{7-\delta}$. We describe the oxygen vacancy reordering by a Monte Carlo simulation of oxygen rearrangement in a layer of Cu-O chains. The "asymmetric next nearest neighbor model" that describes the oxygen ordering phase diagram was combined with next-nearest neighbor hopping rules (Kawasaki dynamics) for oxygen atoms in the plane. The interaction parameters V_1–V_4 are as defined in Ref. 22. A more detailed description of the simulation can be found in Ref. 13. Here and

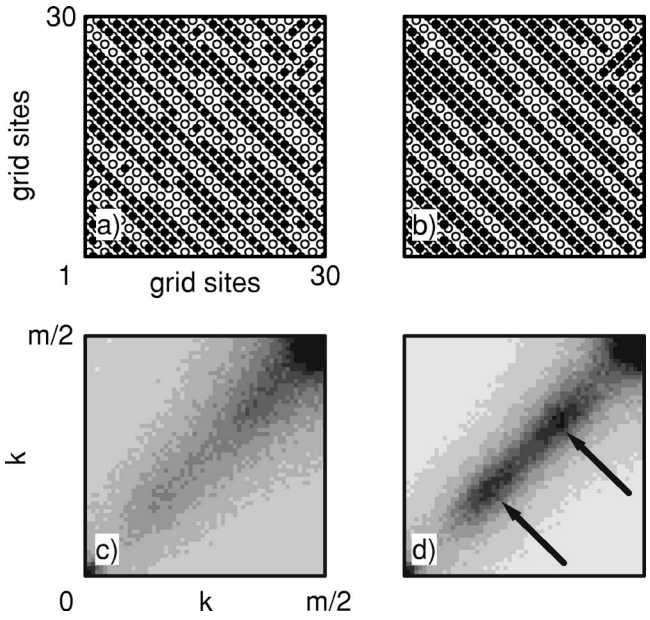

FIG. 4. (a),(b) Monte Carlo simulation of oxygen diffusion in a chain plane with concentration 0.66 in real space, with the crystallographic axes running along the diagonals (open symbols represent Cu atoms, full symbols O), (c),(d) and after two dimensional discrete fast Fourier transform ($m=1200$) (a) and (c) correspond to the state after annealing at 1000 K, (b) and (d) after subsequent quenching and annealing at 350 K. Note the appearance of the two superstructure peaks corresponding to the ortho-III phase (arrows).

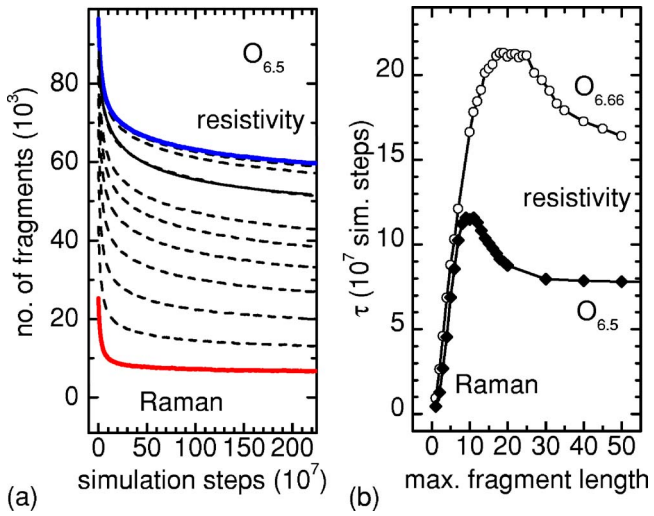

FIG. 5. (Color online) (a) Number of chain fragments versus simulation steps by length, taken from the matrix with oxygen content 0.5. The lowest curve represents single oxygen atoms and corresponds closest to the Raman signal (red), the uppermost line represents all fragments regardless of length and is related to the resistivity in our model (blue). In between are length 1+2, 1 and 3, 1 and 4, etc. A fit example to the fourth curve from the top is also shown. (b) Extracted time constants, full symbols correspond to oxygen content 0.5, open symbols to 0.66.

in this reference we define temperature by the relation of $100\times10^{-3}V_1/k_B=543$ K. In the two simulation runs presented, we equilibrated a 1200 by 1200 site matrix at 1000 K, well into the tetragonal region of the structural phase diagram, with oxygen filling factors of 0.50 and 0.66, respectively. Then we quenched the matrix to 350 K, where we monitored the development of chain fragments of different length. At lower temperatures, a more ordered chain pattern with longer fragments is expected. In the case of low oxygen filling (0.5), which corresponds to our sample, a superstructure cell emerges with a pattern of alternating full and empty chains perpendicular to the chain direction (ortho-II), while the higher oxygen filling (0.66) develops a more complicated pattern with two full and one empty chain (ortho-III).

Figure 4 illustrates a part of the matrix with 0.66 before and after chain fragment development at 350 K. The *a* and *b* axes of the unit cell run at 45° to the picture boundaries. During annealing at 350 K, the disorder with a high number of short chain fragments in (a) vanishes in favor of longer fragments (b). A pattern has developed in which two oxygen-filled chains alternate with one empty chain. In Fig. 4(c) and 4(d) the Fourier transform is displayed, illustrating the corresponding increase of ortho-III signal at one third and two thirds of the diagonal (arrows).

The reordering of chains into longer fragments and regular patterns is known from thermal annealing of oxygen-deficient $YBa_2Cu_3O_{7-\delta}$.[23] Its effect on conductivity comes from the ability of the chain-Cu atoms to dope the superconducting planes depending on their oxygen coordination number.[24] In this picture, an average of twofold (no chain) and fourfold (within chain) coordinated Cu atoms provides higher hole doping to the planes than the same ensemble of threefold (chain-end) coordinated Cu atoms, though the total number of oxygen atoms in the plane remains unaltered. Resistivity is thus sensitive to a change of the average Cu coordination number, or average fragment length, correspondingly. The forbidden Raman scattering signal, on the other hand, from the results of a cluster calculation is attributed to a resonant electronic excitation at a short chain fragment.[8] The Raman intensity should therefore be high for a large number of short fragments and decrease as annealing into longer chains occurs. It is assumed to be proportional to the density of resonance excitation centers in the chain plane, as nonlinear effects can be excluded from previous results.[25]

Microscopically, the observed annealing of shorter fragments into longer Cu-O chains has different effects on the Raman scattering signal and on the transport measurements: Raman is more sensitive to the quickly vanishing shorter fragments, while the increase in carrier concentration is driven by the slower change of average Cu coordination. Figure 5 illustrates the idea. The left panel shows the number of fragments in an oxygen matrix versus simulation time with the fragment length as a parameter. The lowest curve represents single oxygens only, the highest the total fragment number of any length. Intermediate curves are also shown (dashed lines). Time constants extracted from both matrices using a stretched exponential fit are displayed in the right panel of Fig. 5. The best fit to all curves with the same β was obtained with $\beta=0.28$. The parameter depends on the temperature difference of the simulated quench and in this case is slightly different from the experimental result, however, no quantitative comparison between experimental and model

time constants is intended. Generally, the time constants are shorter for the matrix with lower oxygen content. Comparison within the time constants for each matrix shows that the short chain fragments—responsible for the Raman signal—decrease about 15–20 times faster than the total number of chain fragments related to the decrease in resistivity for both oxygen contents tested. We can thus ascribe the two seemingly different experimental time constants to two aspects of the same microscopic chain ordering process. We note that this difference is not critically dependent on the oxygen content between 6.5 and 6.66, or on the type of superstructure pattern.

Remarkably, the slowest decrease occurs for intermediate chain length. This is related to the fact that short fragments simply disappear and long fragments continuously grow. Intermediate curves, however, result from a balance between creation and destruction, which gives them longer lifetime.

Another similarity we note is that of fast Raman bleaching and the fast response of the carrier mobility under illumination. Hall measurements in Ref. 1 have shown that both carrier concentration and mobility increase under illumination. We estimate from the data that mobility reacts faster than carrier concentration by about two orders of magnitude, putting it into the same range of time constants as Raman bleaching. It is plausible that short chain fragments act as scattering centers for the carriers, so that a rapid decrease of their number under illumination could explain the mobility increase observed. Systematic Hall measurements during thermal annealing, under illumination and during relaxation after illumination have shown that photo-excitation has a stronger effect on carrier mobility than annealing, and also that its relaxation is thermally driven.[17] The latter finding supports the idea that oxygens have been displaced by illumination. The fast response of mobility to light indicates that the situation is more complex than in thermal annealing only. Illumination is not only pushing the system towards a new equilibrium point, it is also altering its character. It would therefore be interesting to extend model calculations to a form where the final state is not identical to a different state of thermal equilibrium, but instead a state in which the number of very short chain fragments should be even more reduced. Raman bleaching and Hall measurements are the corresponding tools for observing the fast and slow elements of the structural change in experiment. Thus, they provide insight into two separate microscopic aspects of persistent photoconductivity.

IV. CONCLUSIONS

We present a simultaneous study of the light-induced effects in underdoped $GdBa_2Cu_3O_{7-\delta}$ known as Raman bleaching and persistent photoconductivity. Despite the fact that the effects are known to display similar properties and do show similar temperature dependences in our study, we also found a clear difference: The characteristic time constant of Raman bleaching is two orders of magnitude faster than the response in electrical resistivity. Similar time scale differences between carrier concentration and mobility provide evidence that Raman response is connected more closely to the mobility than to the overall electrical conductivity.

We discuss our findings within the model of oxygen-vacancy reordering, using a Monte Carlo simulation of chain-fragment development after a temperature quench. In this picture, Raman response is connected to the number of short fragments, which react quickly to the new equilibrium conditions. Electrical conductivity, on the other hand, senses the slower change of average Cu coordination numbers. We are thus able to show that Raman bleaching and persistent photoconductivity are connected to the same microscopical origin of oxygen reordering and yet display different characteristic time constants.

The results presented here show that the observed properties are consistently explained within an oxygen reordering model, though they do not provide exclusive evidence for one of the models discussed in persistent photoconductivity. However, the experiment and proposed interpretation yield a more complete picture of the persistent photo-excitation effects. The long-standing assumption that Raman bleaching and persistent photoconductivity are two sides of the same light-induced change in the underdoped $RBa_2Cu_3O_{7-\delta}$ material family must be altered: The optical and electrical response are connected, but not identical. Their comparison can yield distinct information on the microscopic properties governing the Raman response, the conductivity, and the carrier mobility.

ACKNOWLEDGMENTS

S.B. thanks C. Kristukat for helpful discussions. S.B. acknowledges funding by the "Berliner Programm für Chancengleichheit von Frauen in Forschung und Lehre." This work was supported jointly by the Deutscher Akademischer Austauschdienst (DAAD) and the Agencia Nacional para la Promoción Científica y Tecnológica of Argentina (ANPCyT) under the program PROALAR 2000.

[1] G. Nieva, E. Osquiguil, J. Guimpel, M. Maenhoudt, B. Wuyts, Y. Bruynseraede, M. B. Maple, and I. K. Schuller, Phys. Rev. B **46**, 14249 (1992).

[2] V. I. Kudinov, I. L. Chaplygin, A. I. Kirilyuk, N. M. Kreines, R. Laiho, E. Lähderanta, and C. Ayache, Phys. Rev. B **47**, 9017 (1993).

[3] J. Guimpel, B. Maiorov, E. Osquiguil, G. Nieva, and F. Pardo, Phys. Rev. B **56**, 3552 (1997).

[4] C. Stockinger, W. Markowitsch, W. Lang, W. Kula, and R. Sobolewski, Phys. Rev. B **57**, 8702 (1998).

[5] W. Markowitsch, A. Altenburger, W. Lang, M. Peruzzi, J. D. Pedarnig, and D. Bäuerle, Physica C **405**, 173 (2004).

[6] J. Hasen, D. Lederman, I. K. Schuller, V. Kudinov, M. Maenhoudt, and Y. Bruynseraede, Phys. Rev. B **51**, 1342 (1995).

[7] D. R. Wake, F. Slakey, M. V. Klein, J. P. Rice, and D. M. Ginsberg, Phys. Rev. Lett. **67**, 3728 (1991).
[8] A. Bruchhausen, S. Bahrs, K. Fleischer, A. R. Goñi, A. Fainstein, G. Nieva, A. A. Aligia, W. Richter, and C. Thomsen, Phys. Rev. B **69**, 224508 (2004).
[9] S. Bahrs, A. R. Goñi, C. Thomsen, B. Maiorov, G. Nieva, and A. Fainstein, Phys. Rev. B **65**, 024522 (2002).
[10] A. G. Panfilov, M. F. Limonov, A. I. Rykov, S. Tajima, and A. Yamanaka, Phys. Rev. B **57**, R5634 (1998).
[11] A. G. Panfilov, A. I. Rykov, S. Tajima, and A. Yamanaka, Phys. Rev. B **58**, 12459 (1998).
[12] C. Thomsen, M. Cardona, B. Gegenheimer, R. Liu, and A. Simon, Phys. Rev. B **37**, R9860 (1988).
[13] S. Bahrs, A. R. Goñi, C. Thomsen, B. Maiorov, G. Nieva, and A. Fainstein, Phys. Rev. B **70**, 014512 (2004).
[14] A. Fainstein, P. Etchegoin, and J. Guimpel, Phys. Rev. B **58**, 9433 (1998).
[15] A. Fainstein, B. Maiorov, J. Guimpel, G. Nieva, and E. Osquiguil, Phys. Rev. B **61**, 4298 (2000).
[16] M. Käll, M. Osada, M. Kakihana, L. Börjesson, T. Frello, J. Madsen, N. H. Andersen, R. Liang, P. Dosanjh, and W. N. Hardy, Phys. Rev. B **57**, R14072 (1998).
[17] B. Maiorov, Master's thesis, Instituto Balseiro, Comisión Nacional de Energía Atómica, 8400 San Carlos de Bariloche, Río Negro, Argentina, 1997.
[18] R. Liu, C. Thomsen, W. Kress, M. Cardona, B. Gegenheimer, F. W. de Wette, J. Prade, A. D. Kulkarni, and U. Schröder, Phys. Rev. B **37**, R7971 (1988).
[19] S. Bahrs *et al.* (unpublished).
[20] H. Scher, M. F. Shlesinger, and J. T. Bendler, Phys. Today **44**, 26 (1991).
[21] A. L. Kotz, M. V. Klein, W. C. Lee, J. Giapintzakis, D. M. Ginsberg, and B. W. Veal, Phys. Rev. B **45**, R2577 (1992).
[22] N. H. Andersen, M. von Zimmermann, T. Frello, M. Käll, D. Mønster, P. A. Lindgård, J. Madsen, T. Niemöller, H. F. Poulsen, O. Schmidt, J. R. Schneider, Th. Wolf, P. Dosanjh, R. Liang, and W. N. Hardy, Physica C **317–318**, 259 (1999).
[23] J. D. Jorgensen, S. Pei, P. Lightfoot, H. Shi, A. P. Paulikas, and B. W. Veal, Physica C **167**, 571 (1990). A. A. Maksimov, D. A. Pronin, S. V. Zaitsev, I. I. Tartakovskii, G. Blumberg, M. V. Klein, M. Karlow, S. L. Cooper, A. P. Paulikas, and B. W. Veal, Phys. Rev. B **54**, R6901 (1996).
[24] A. A. Aligia and J. Garcés, Phys. Rev. B **49**, 524 (1994).
[25] Raman studies concluded that both the intensity and the decrease of defect-induced peaks scale linearly with the excitation power (see Refs. 7 and 10). Furthermore, the electronic excitation which is responsible for the resonant scattering of the defect-induced modes is rather broad [full width at half maximum 160 meV (see Ref. 7)] and the corresponding feature in reflectance anisotropy decreases under illumination, but does not shift in energy (see Ref. 8).